Supplementary Materials for

Redox-active antibiotics enhance phosphorus bioavailability

Darcy L. McRose and Dianne K. Newman*

*Corresponding author. Email: dkn@caltech.edu

Published 5 March 2021, *Science* **371**, 1033 (2021)
DOI: 10.1126/science.abd1515

This PDF file includes:

Other Supplementary Material for this manuscript includes the following:
(available at science.sciencemag.org/content/371/6533/1033/suppl/DC1)

MDAR Reproducibility Checklist

Materials and Methods:

Phylogenetic tree construction

Small subunit ribosomal RNA sequences (242 total) were downloaded from SILVA (*34*). Species that produce antibiotics in response to P limitation and those in which *phoB/P* or *phoR* regulation has been shown are typically represented at the species level because sequences were not available for all specific strains, and in the case of some *Actinobacteria* and *Firmicutes* the exact strain used in experiments could not be always be identified from literature citations. See Table S1 for citations and details. Sequences were aligned with the SINA aligner (*35*) and a phylogenetic tree was constructed with RAxML (*33*) and rendered in iTOL (*36*).

Continuous culture conditions

Wild type strains of *Pseudomonas aeruginosa* UCBPP-PA14, *Pseudomonas aureofaciens* 30-84, *Pseudomonas fluorescens* 2-79, *Pseudomonas chlororaphis* PCL1391, *Burkholderia thailandensis* E264, and *Serratia* ATCC39006 (formerly *S. marcescens*) were grown in defined medium containing: 4.1 x 10^{-4} M $MgSO_4 \cdot 7H_2O$, 6.8 x 10^{-4} M $CaCl_2 \cdot 2H_2O$ and either 4 x 10^{-2} M glucose (*P. aureofaciens, P. fluorescens, P. chlororaphis,* and *B. thailandensis*), succinate (*P. aeruginosa*), or glycerol (*Serratia* ATCC39006) as the carbon source. Phosphate-limited cultures were supplied with 1.6 x 10^{-2} M NH_4Cl, 7.3 x 10^{-6} M KH_2PO_4 and 3.4 x 10^{-6} M K_2HPO_4 (16 mM N, 10 µM total P). Nitrogen limited cultures were supplied with 2 x 10^{-4} M NH_4Cl, 4.7 x 10^{-3} M KH_2PO_4, and 2.3 x 10^{-3} M K_2HPO_4 (200 µM N, 7 mM total P). A modified version of Aquil trace metals (*37*) containing 1 x 10^{-5} M Fe and 1 x 10^{-4} M EDTA was also added. The medium was buffered at pH 7 with 25 or 50 mM MOPS. N- and P-limited media were designed assuming cellular quotas were roughly Redfieldian (*38*) and were refined empirically to yield a max OD500 of ~ 0.1 under both conditions (200 µM N and 10 µM P yielded approximately equal ODs, N:P of 20). The growth medium was prepared in acid-cleaned bottles and sterilized via filtration (Stericup, Millipore Sigma). Cultures were maintained as freezer stocks, streaked onto LB plates and then grown overnight in experimental medium before the start of experiments, conducted using a Sartorius Biostat QPlus chemostat system. The entire chemostat system including all tubing and sensors was assembled and autoclaved, ~500 mL of growth medium was then pumped into sterile vessels. Experiments commenced with the inoculation of ~60 mL of overnight culture and were conducted at 30°C (*P. aureofaciens, P. fluorescens P. chlororaphis, B. thailandensis*, *Serratia* ATCC39006) or 37°C (*P. aeruginosa*) with constant aeration and mixing. Chemostats were allowed to equilibrate at each dilution rate until pH, redox, and O_2 were stable (generally ≥ 12 hours) before sampling. Aliquots were withdrawn aseptically and OD at 500 nm was measured by spectrophotometry (Beckman DU 640). Dilution rates were determined using the medium flow rate and the exact culture vessel volume (determined gravimetrically at the end of each experiment) and are considered equivalent to growth rates (µ) at steady state.

For metabolite detection, 1 mL of culture was centrifuged, the supernatant was filtered (0.22 µm, Corning Costar Spin-X centrifuge filter) and frozen for later analysis. To quantify prodigiosin, which is cell associated, *Serratia* cell pellets were extracted overnight in ethanol+0.1% formic acid, reported concentrations are normalized assuming $1x10^9$ cell mL^{-1} OD^{-1}. Phenazines were measured using a Waters LC-MS (Waters e2695 Separations Module fitted with 2998 PDA Detector) on a C18 column (XBridge, 3.5 µm, 2.1 x 50 mm) at a flow rate of 0.5 mL min^{-1} with a gradient of water + 0.04% NH_4OH to 70% acetonitrile + 0.04% NH_4OH with a constant

background of 2% methanol over 20 minutes. Concentrations were determined using the extracted absorbance at 364 nm and comparison to a standard curve. Prodigiosin and bactobolin were detected using a Quadrupole Time of Flight MS (Q-TOF, Xevo G2-XS, Waters) with a C18 column (Waters Acquity CSH, 1.7 µm, 2.1 x 100 mm). Samples were run with a gradient of water + 0.1% formic acid to acetonitrile + 0.1% formic acid at a flow rate of 0.4 mL min^{-1} over 5 minutes. Prodigiosin identity and concentration was determined by comparison to a standard curve. Bactobolin identity was confirmed via MS/MS targeting m/z 383.1 (bactobolin A) and m/z 454.1 (bactobolin B), column and run conditions were as above. We observed parent masses of m/z 383.0837 and m/z 454.1268 both with a fragment ion of m/z 312.0504, in agreement with (*39*).

Strain construction

To construct unmarked deletions of *phoB* in *Pseudomonas fluorescens* 2-79 and *Pseudomonas chlororaphis* PCL1391, ~1 kb fragments upstream and downstream of *phoB* were PCR amplified, joined with the suicide vector pMQ30 (*40*) (digested with SacI and HindII) via Gibson assembly (*41*) and electroporated into *E. coli* DH10B. Transformants were plated on LB with gentamicin (20 µg mL^{-1}). The presence of the correct construct was verified via PCR and was introduced into *Pseudomonas* wild type strains using triparental conjugation. Merodiploid transformants were selected on Vogel-Bonner medium (VBMM, (*42*)) containing gentamicin (20 µg mL^{-1}) followed by counter selection on sucrose medium (5 g L^{-1} yeast extract, 10 g L^{-1} tryptone, 100 g L^{-1} sucrose). Colonies in which homologous recombination was successful were identified via PCR.

P. fluorescens and *P. chlororaphis* were complemented using the method described by (*42*). The deleted locus as well as a 200 base pairs upstream region containing a predicted PHO box and the downstream intergenic region was amplified by PCR and joined with the shuttle vector pUC18T-mini-Tn*7*T (digested with SacI and HindII) via Gibson assembly and introduced into *E. coli* DH10B via electroporation. Transformants were plated on LB containing gentamicin (20 µg mL^{-1}). The appropriate complementation construct was introduced into *P. fluorescens* and *P. chlororaphis phoB* mutants via tetraparental conjugation. Conjugants were selected on VBMM medium containing gentamicin (20 µg mL^{-1}). The integration of the complemented *phoB* sequence at the chromosomal *att*Tn7 site was verified using two sets of PCR primers designed to *glmS* (see (*42*)) and to *phoB*.

Abiotic experiments

Two-line ferrihydrite (herein hydrous ferric oxide, HFO) was synthetized by rapid addition of KOH to $Fe(NO_3)_3$ as described by (*43*). Fe precipitates were concentrated via centrifugation (30 min at 18,000 *x* g) and then dialyzed for 4 days, collected by centrifugation (30 min at 18,000 *x* g), air dried, and stored at -80°C. X-ray diffraction analysis showed two broad peaks at 2.6 and 1.7 Å, consistent with 2-line ferrihydrite (data not shown). For phosphate adsorption, 80 mg of HFO was incubated for a minimum of 48 hours in 50 mL of 20 mM K_2HPO_4 adjusted to pH 6. Incubations were performed in an O_2-free chamber (Coy laboratory products). Preliminary experiments suggested that the majority of P adsorption occurred within 48 hours and ~1.2-1.8 mmole of phosphate was adsorbed g^{-1} HFO (Fig. S3). Owing to the inherent heterogeneity of amorphous Fe oxides, phosphate adsorption can vary greatly, but these findings are consistent with those from similar studies (for example, (*44, 45*)). At the start of experiments phosphated HFO (HFO-P) particles were pelleted (10 min at 6,800 *x* g), washed twice with 10 mM KCl at pH 6, re-suspended in 40 mL of 10 mM KCl, and aliquoted for experimental manipulations. Reduced

phenazines were obtained via reduction with hydrogen and palladium. Experiments commenced with the addition of reduced phenazines (100 µM final concentration). After 5 hours of incubation, a 1 mL sample was withdrawn, HFO-P particles were pelleted (13000 *x* g for 5 mins) and supernatants were filtered (0.22 µm, Corning Costar Spin-X centrifuge filter). Soluble phosphorus was determined using Inductively Coupled Plasma Mass Spectrometry (Agilent 8800 Triple Quadrupole ICP-MS) run in mass shift mode. Concentrations were determined by comparison to a standard curve. Fe(II) was measured using the Ferrozine assay (*46*). 2 mM Ferrozine was prepared in 100 mM HEPES at pH 6 and mixed with samples and standards. Color was developed for 1 hour at 37 °C before measurements of absorbance at 562 nm. Experiments were carried out using a BioTek Synergy 4 plate reader housed inside an anoxic chamber.

P. aeruginosa and *D. japonica* growth on HFO-P

For analysis of *Pseudomonas* growth on HFO-P with exogenous phenazines, a *Pseudomonas aeruginosa* mutant unable to make phenazines (Δ*phzA-G1,* Δ*phzA-G2 (47))* was grown in P-free succinate medium (described above except: 20 mM KNO_3 was added instead of NH_4Cl, MOPS was omitted, and Fe was added as 5 µM $FeCl_2$). Cells were acclimated to denitrifying conditions by overnight growth in an anoxic chamber in the described nitrate rich medium. At the start of experiments, cells were inoculated into experimental treatments and grown at 37˚C with constant shaking in a plate reader inside an anoxic chamber. Growth was tracked using absorbance measurements at 500 nm taken every hour. The preparation of HFO-P was similar to that for abiotic experiments. Briefly, 80 mg HFO was equilibrated under anoxic conditions for >48 hours in 40 mL of solution containing 20 mM K_2HPO_4 and 10 mM KCl, adjusted to pH 6. This slurry was centrifuged (10,000 *x g* for 10 minutes), washed once with pH 6 KCl, centrifuged again and diluted 4X in P-free medium, 10 mL aliquots of the resulting slurry were used to create various experimental treatments and final growth experiments were conducted using 200 µL aliquots. P (when added) was added at a final concentration of 7 mM.

For experiments testing the growth benefits of endogenous phenazine production, the wild type strains *P. aeruginosa* UCBPP-PA14 and *Dyella japonica* UNC79MFTsu3.2 as well as mutant strains unable to make phenazines: *P. aeruginosa* Δ*phzA-G1,* Δ*phzA-G2* (47) and *D. japonica* Δ*phzT* (*27*) were acclimated for 24 (*P. aeruginosa*) or 48 (*D. japonica*) hours in P-limited (10µM P) medium and then inoculated into acid-cleaned glass test tubes at an OD of 0.03 (*P. aeruginosa*) or 0.05-0.06 (*D. japonica*) in a 5 mL volume. Growth medium for *P. aeruginosa* was the same as used in continuous culture experiments only without MOPS or EDTA. *D. japonica* was grown with glucose as the carbon source (as described for continuous culture experiments) but with the addition of MEM essential amino acids (Sigma, M5550) and the omission of MOPS and EDTA. For *D. japonica,* plate reader experiments were also conducted under P replete conditions without HFO-P (Fig. S2C), here the growth medium was as described for P-replete continuous culture experiments with glucose as the carbon source, plus MEM amino acids and 5 mM ammonium.

HFO-P preparation was similar to that described above: particles were centrifuged, washed once with KCl, and diluted 4X in a growth medium without any added phosphate, 10 µM Fe (as $FeCl_3$) was added immediately before experiments commenced. For high P experiments, phosphate was added at a final concentration of 1 mM immediately before the start of experiments. Cultures were grown at either 30˚C (*D. japonica*) or 37˚C (*P. aeruginosa*) and shaken at 250 rpm in ambient O_2 conditions. At each time point, cultures were vortexed and optical density was measured via absorbance at 500 nm. Following this, cultures were allowed to sit statically for 1 hour and 300 µL (without agitation) was withdrawn for Fe(II) measurements via the Ferrozine

assay. Samples were centrifuged and 0.2 µm filtered before being assayed. Sampling was conducted in ambient air but centrifugation, filtration, and Ferrozine assays were conducted in an anoxic Coy chamber. The phenazine pyocyanin has an absorbance that overlaps with the Fe(II) Ferrozine complex (562 nm) and while slight elevation in absorbance at 562 nm was observed in *P. aeruginosa* wild type cultures, it was not significantly higher than that of control samples run in HEPES buffer without Ferrozine, thus while modest Fe(II) accumulation may occur in these samples, it is likely minimal (a few micromolar at most). In contrast, Fe(II) clearly accumulated in *D. japonica* supernatants (Fig. S2A).

Phenazine production was visibly detectable in wild type cultures of both species and was verified by LC-MS. For *P. aeruginosa* pyocyanin was detected by LC-MS (as described above) and verified with a standard. For *D. japonica*, the presence of myxin (*m/z* 259.1) and a myxin derivative with m/z 243.1 was confirmed via the presence of the expected masses accompanied by a characteristic absorbance signal at 280 nm and the absence of these masses in mutant supernatants. LC-MS conditions for myxin were as stated for other phenazines, only acidic (0.1% formic acid) water (as buffer A) and acetonitrile (as buffer B) were used. Notably, while pyocyanin was detected throughout growth, myxin was only detected at early time points; the myxin derivative was observed throughout experiments, possibly in keeping with the scheme proposed by (*48*) where hypoxic conditions permit the full conversion of myxin through a radical intermediate to the derivative *m/z* 243.1.

D. japonica experiments were highly sensitive to initial starting conditions and small differences in the inoculum used in pre-growth affected the extent of the advantage conveyed by phenazine production (compare Fig. 3C, Fig. S2B). Like other phenazines, myxin and its derivatives should generate reactive oxygen species (ROS) via Fenton chemistry, which would be expected to occur in the presence of Fe-oxides. Potential phenazine toxicity may in fact be reflected in Fig. S2B where phenazine mutants show a growth advantage in P-replete conditions with HFO-P. As such, the benefits of P acquisition afforded by phenazine production (not just for *D. japonica* but also for *P. aeruginosa*) may be tempered by the effects of ROS. Secondary metabolite production in *D. japonica* is also not as well studied as it is in *P. aeruginosa*, and it appears that the *D. japonica* phenazine mutants may still make a reductant (note Fe(II) accumulations in *phzT* mutants, Fig. S2A). Given this, our observations of enhanced growth in the wild type may actually underestimate the effect. It is also notable that the conversion of myxin to its derivative *m/z* 243.1 is reportedly sensitive to oxygen tensions (*48*), with a radical intermediate molecule being oxidized back to myxin when oxygen is high and fully converted to the derivative when oxygen is low. Thus, small changes in cell density and/or respiration rates might disproportionately affect which phenazines are present and the ways in which they react with Fe-oxides, possibly leading to the experimental variability that we observe.

<u>Environmental sample collection and manipulations</u>

Soils from a visibly iron-rich bank on Catalina Island and adjacent seawater were collected from 33° 26.1008' N, 118° 30.1868' W on August 6th 2019 (Site 1). Sediments and overlying water samples were also collected from Catalina Island on August 6th and October 22nd, 2019 at 33° 25.7952' N, 118° 30.2765' (Site 2). Samples from Site 1 were maintained at 21°C for 9 days before being aliquoted into serum vials. Following collection, samples from Site 2 were immediately homogenized and 1 g of sediment was placed into sterile, acid cleaned serum vials and covered with 25 mL site water. After sediment/soil additions to serum vials, all samples were incubated overnight at 21°C, sparged with N_2 gas and incubated overnight again before the addition of

reduced or oxidized phenazines (100 µM final concentration). Phenazine solutions were prepared in 10 mM KCl at pH 7 and made anoxic via sparging with N_2. Reduced phenazines were obtained using either hydrogen and palladium (August experiments) or controlled potential bulk electrolysis (October experiments) and were sparged with N_2 before being used for experiments. KCl solution was added to control experiments to account for changes in volume. For ethanol killed experiments, sediments were soaked in 70% ethanol. After 24 hours, ethanol was decanted and lyophilized. To ensure that any organic compounds that might have been extracted in the ethanol were not lost (thus potentially biasing the experiment) the vessel used for lyophilization was rinsed with a small volume of overlying water which was then added back to serum vials (for a total of 25 mL overlying water). Vials were then treated as above. All sampling was conducted in an anoxic chamber. Briefly, 1 mL of sediments slurry was withdrawn with a syringe and samples were treated as in abiotic experiments (centrifugation followed by filtration). For measurements of reduced PCA, the filtration steps were excluded as preliminary experiments showed retention of phenazines on 0.22 µm filters. Instead, samples were pelleted and reduced PCA in supernatants was quantified immediately via fluorescence (*49*) using a plate reader (BioTek Synergy 4) inside an anoxic chamber. Soluble phosphorus was determined by ICP-MS and Fe(II) was measured using the Ferrozine assay (described above). Sulfide was tested at the end of experiments using the Cline assay (data not shown (*50*)). Briefly: to precipitate sulfide, 500 µL of sediment slurry was mixed with 500 µL of 500 mM zinc acetate dihydrate and samples were stored for later analysis. Preserved sediment slurries were then mixed with N,N-dimethyl-p-phenylenediamine dihydrochloride (0.5 mM final concentration) and $FeCl_3 \cdot 6H_2O$ (1.2 mM final concentration) and color formation was tracked via absorbance at 670 nm on a BioTek Synergy 4 plate reader.

For carbon manipulation experiments, samples collected on Oct 22, 2019 at Site 2 were sparged with N_2 as above and incubated at 21°C for 2 weeks without any additions. At this time, samples were treated with i) a mixture of glucose and lactate (10 mM final concentration of each) and oxidized PCA (100 µM final concentration) or ii) oxidized PCA (100 µM final concentration) alone. The accumulation of reduced PCA was determined as described above. Abiotic control experiments were also conducted without sediments but with filtered overlying water, glucose and lactate, as well as oxidized PCA, and did not show any PCA reduction. Sulfide was tested in these experiments (as above) and was not detected, suggesting SRB were not involved in PCA reduction.

For extractable iron and phosphorus concentrations, sediments were dried at 50°C until they obtained a stable mass and subsequently homogenized with a mortar and pestle. 1 g of dry soil was placed in a polypropylene DigiTUBE (SCP science) with 5 mL undiluted nitric acid and incubated on a hot plate at 95°C for 6 hours. Supernatants were decanted, diluted, filtered and analyzed by ICP-MS (phosphorus as above, iron also in mass shift mode). Iron and phosphorus concentrations in nitric acid blanks passed through the same digestion process were below detection limits (~ 2 ppb for Fe, ~ 1 ppb for P) and samples spiked with phosphorus showed a recovery of 117% ± 0.1% across triplicates (recoveries >100% are likely due to slight evaporation during hot plate digestion). Overlying water samples were diluted 20-fold and analyzed directly with MS methods described above and P concentrations were <0.5 µM for all sites.

Statistical analyses

All statistical tests were conducted using R (*51*). Data normality was verified with the Shapiro-Wilk normality test. We checked for significant differences between soluble phosphorus

concentration at the initial time point in each experiment using a one-way ANOVA (aov function, soluble phosphate ~ treatment). Ethanol treatments from Site 2, sampled in October (biological suppression experiments) showed significantly higher initial phosphorus levels ($p \leq 0.01$) and were excluded from further phosphorus analysis. The evolution of phosphorus over time for each replicate was then calculated by difference to the initial time point (Figs. 4, S4). For phosphorus solubilization, where we had no clear expectation of evolution over time, one-way ANOVA tests (aov function, soluble phosphate ~ treatment) with Tukey posthoc corrections (TukeyHSD, confidence.level=0.95) were conducted across treatments (all treatments shown in Fig. S4) at each time point, *p* values are indicated on Figs. 4, S4. If this analysis is conducted as a two-way ANOVA for treatment by time (treatment*time), differences indicated on Figs. 4, S4 are still significant ($p<0.1$ for the 5-hour time point in Site 2 August experiments, $p<0.05 – p< 0.0001$ for 144-336 hour time points in October experiments). For biological stimulation and suppression experiments (Fig. 4E,F) *p*-values reported are for two-way ANOVA of treatment*time with Tukey posthoc corrections.

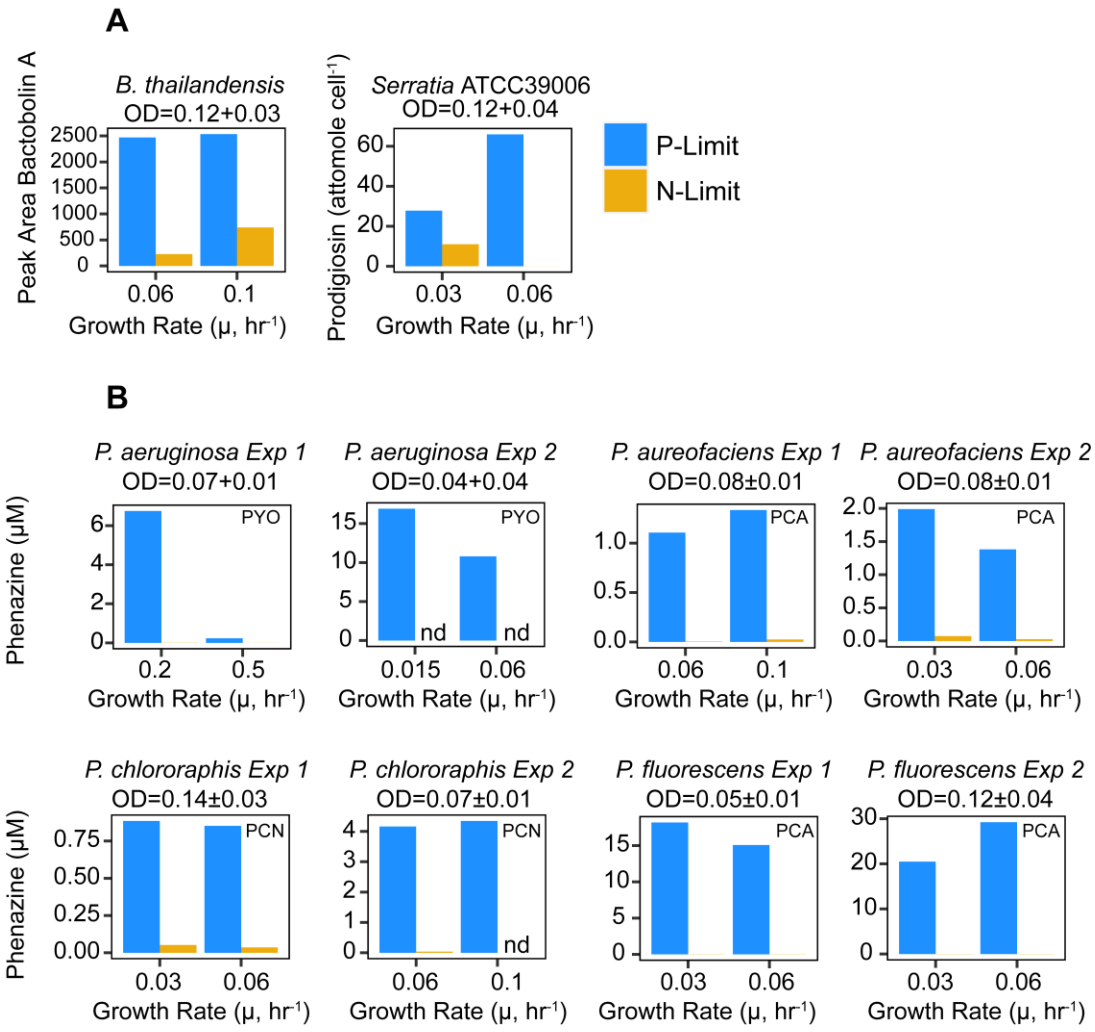

Fig. S1. Chemostat experiments. (A) Chemostat experiments with *Burkholderia thailandensis* E264 suggest that bactobolin production is regulated by phosphate in this organism. Data reported are for bactobolin A, but bactobolin B was also detected and showed similar trends (data not shown). Consistent with previous studies (*52, 53*) prodigiosin production in *Serratia* ATCC39006 is increased under phosphate limitation. **(B)** *Pseudomonas* chemostat experiments. Data from Experiment 2 are the same as **Fig. 2A.** Reported growth rate (μ) is the dilution rate, the two are equivalent at steady state. The range of ODs across chemostats for each experiment ± standard deviation is listed. Previous studies have reported an effect of growth rate on phenazine production in *P. aeruginosa* (*4, 21*). Initial (Exp 1) experiments with *P. chlororaphis* utilized 50 mM MOPS, which exhibited slight toxicity and was reduced to 25 mM in later experiments, possibly explaining the differences in PCN concentrations between experiments with this organism. Phenazines produced are PCA: phenazine-1-carboxylic-acid; PCN: phenazine-1-carboxamide; PYO: pyocyanin. P: phosphorus (as phosphate), N: nitrogen (as ammonium). nd: not detected.

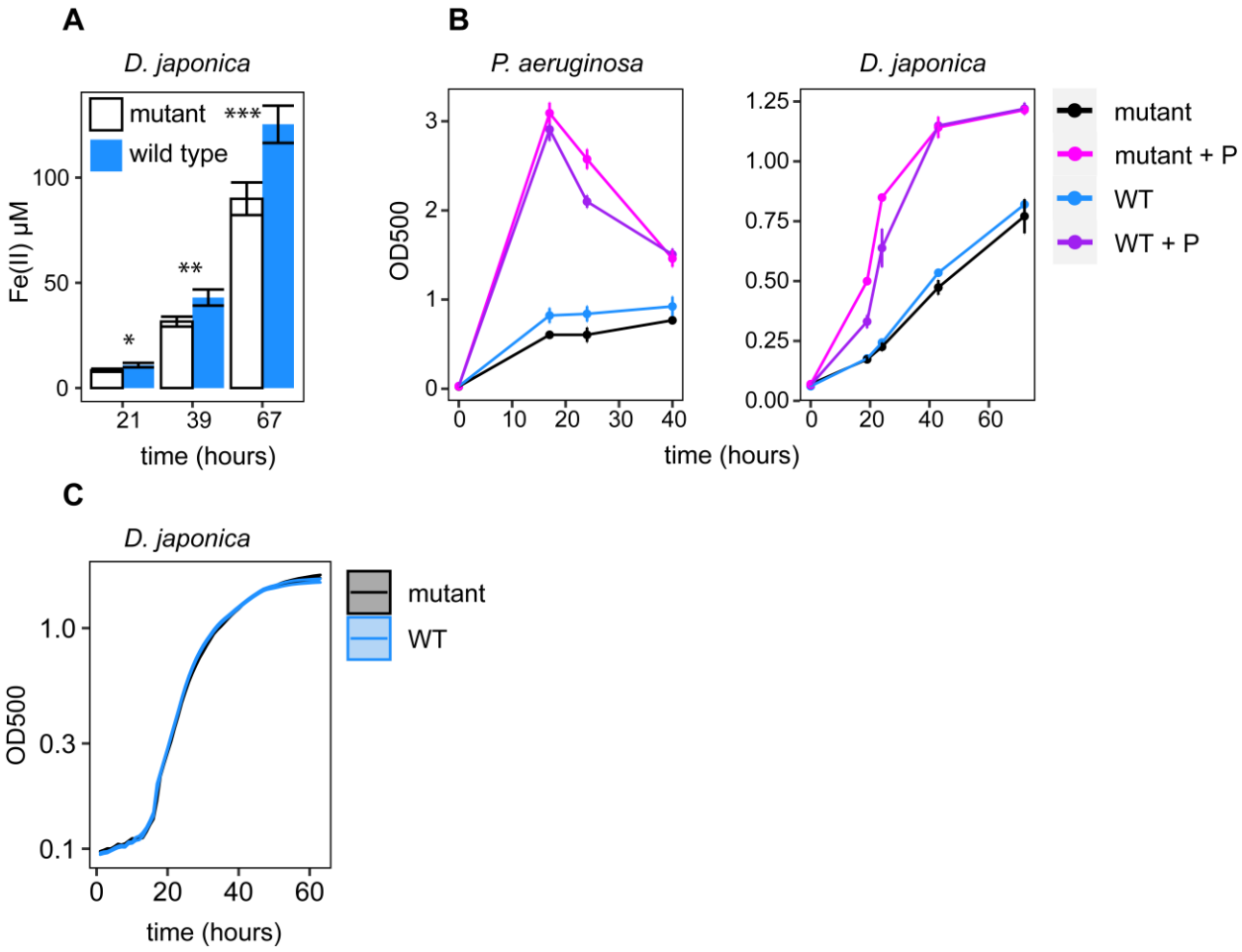

Figure S2. **Growth of *P. aeruginosa* and *D. japonica* wild type and phenazine null mutants.** **(A)** Fe(II) accumulations in *D. japonica* wild type and mutant supernatants. Data correspond to growth experiments shown in **Fig. 3C**. Fe(II) was also measured in *P. aeruginosa* supernatants but was negligible (see Methods). Significant differences for two-tailed t-tests are shown: *$p<0.05$,**$p<0.005$,***$p<0.001$ **(B)** Growth of wild type and mutant strains on HFO-P (blue, black lines) and HFO-P with 1mM added phosphate (purple, pink lines), demonstrating P limitation. For *P. aeruginosa*, HFO-P data are the same as **Fig. 3C**. *Dyella* data represent a replicate experiment and demonstrate the variability of the growth advantage observed in the wild type (compare with **Fig. 3C**, see Methods). **(C)** Growth of *D. japonica* wild type and mutant strains (plate reader data, average ± SD of 5 replicates) in P-replete medium without HFO-P reveal no inherent growth difference between the strains.

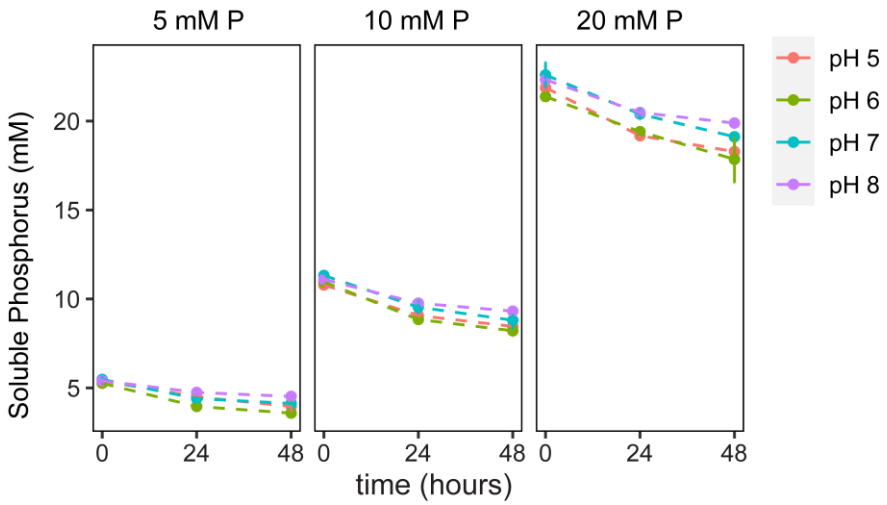

Fig. S3. Preliminary phosphate adsorption experiments. Adsorption of different concentrations of phosphate at pH 5-8. Experiments were conducted in 10 mM KCl with the indicated amount phosphate (as K_2HPO_4) at pH 5-8. Buffers were not used due to concerns about interference with adsorption and downstream reductive dissolution experiments. Soluble P (0.22 µm filtered) was measured by ICP-MS. Experiments were conducted with 10 mg HFO in 5 mL of 10 mM KCl. In our 20 mM phosphate incubations ~1.2-1.8 mmole P was absorbed g^{-1} HFO, which is consistent with other studies (*44*, *45*).

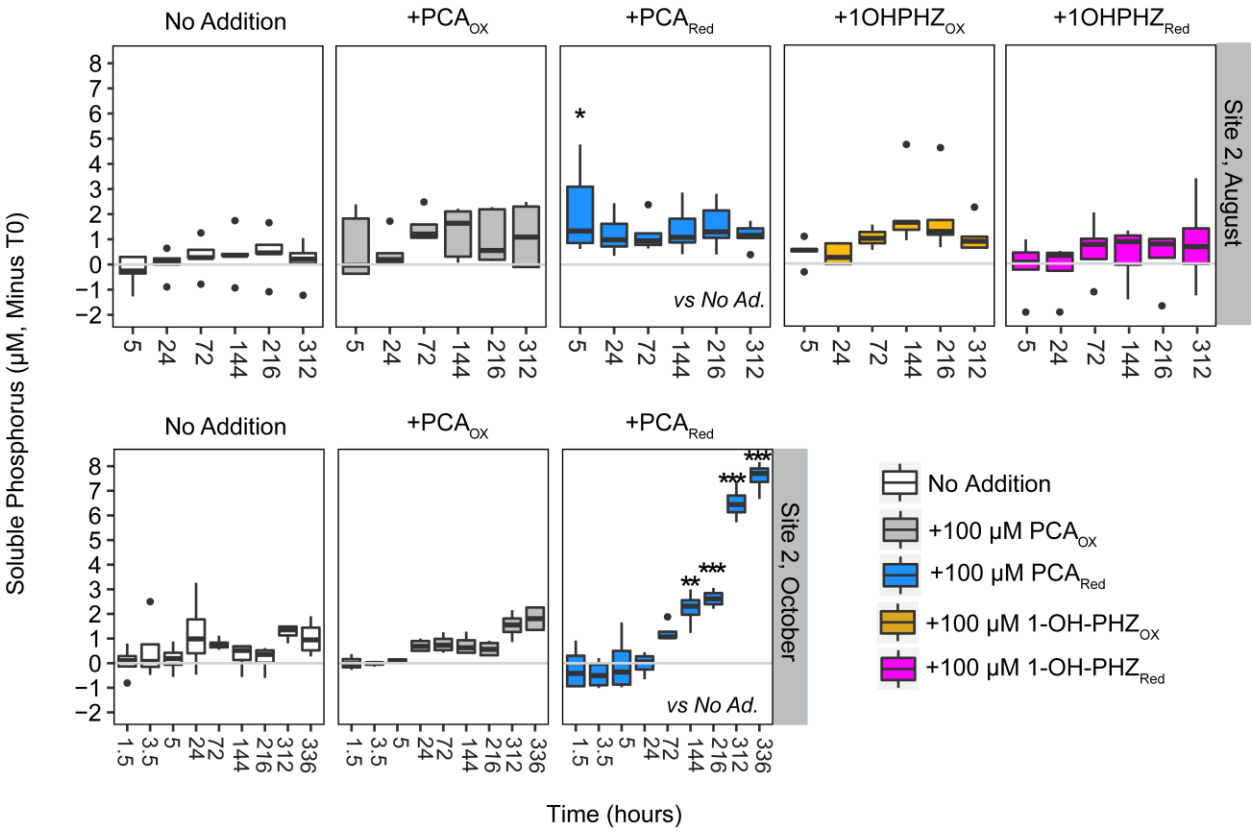

Fig. S4. Phenazines solubilize P in marine sediments. Phosphorus solubilization in Catalina Island sediments incubated with oxidized PCA, reduced PCA, oxidized 1-OH-PHZ, reduced 1-OH-PHZ, or no addition. Data correspond to experiments conducted using sediments from Site 2 collected in August and October. Y-axis corresponds to the difference in total phosphorus (ICP-MS) from the initial time point, grey lines depicts no change. See **Fig. S5** for raw phosphorus data. Plots reflect data from 4 or 5 replicates, data points >1.5x the interquartile range are represented as single black dots. A one-way ANOVA was conducted across all treatments (see Methods) at each time point. For clarity, only significant differences between the control (no addition) and treatments are indicated on the figure. * *p<0.05*, ** *p<0.005*, ***, *p<0.0001*.

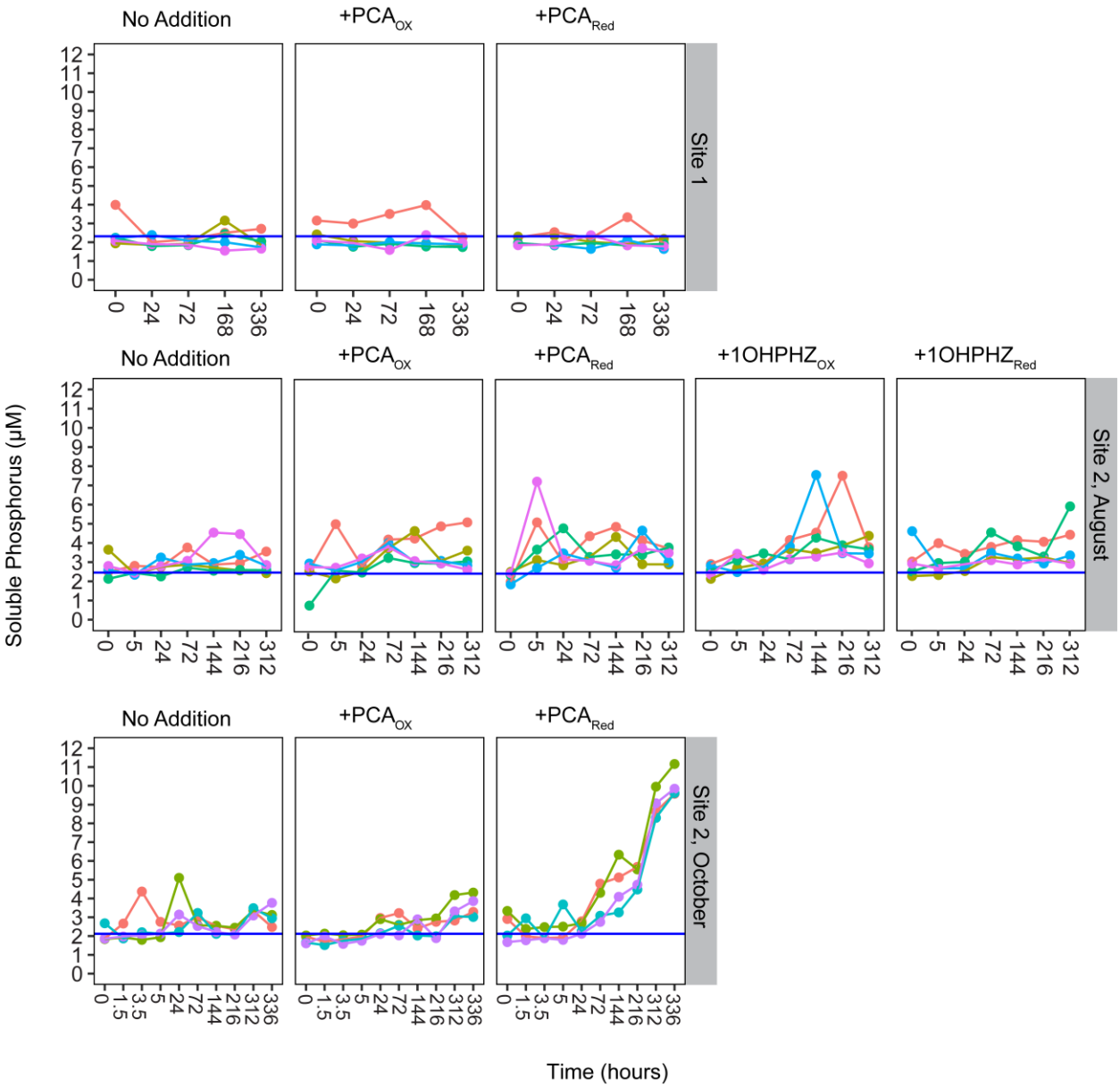

Fig. S5. Soluble phosphorus accumulations in Catalina Island sediments. Total soluble (0.22 μm filtered) phosphorus from Catalina Island sediments incubated with oxidized PCA, reduced PCA, oxidized 1-OH-PHZ, reduced 1-OH-PHZ, or no addition. Data correspond to experiments conducted using sediments from Site 1 collected in August or from Site 2 collected in August and October. Colors indicate different replicates and are arbitrary. Blue line indicates the average phosphorus concentration at time zero for each experiment.

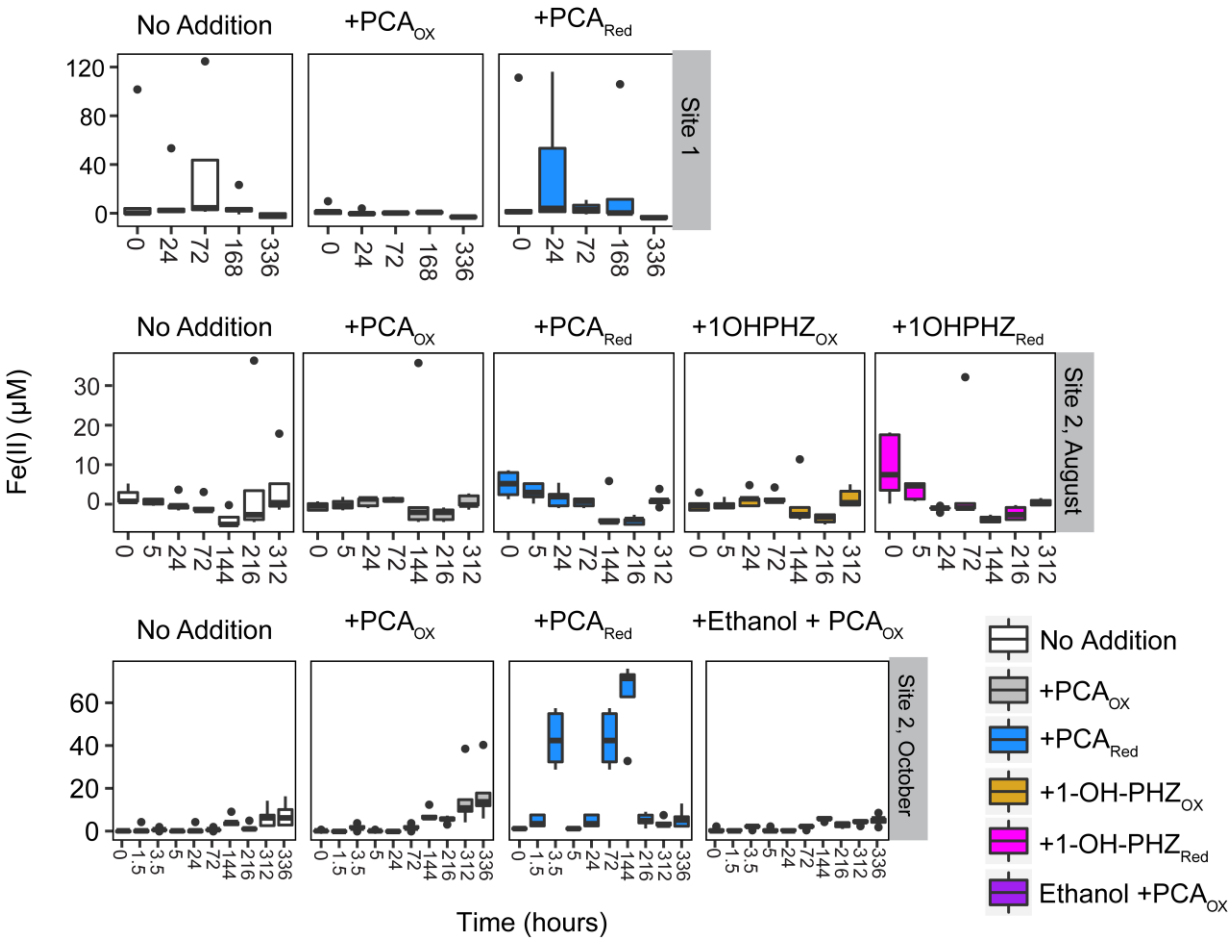

Fig. S6. Soluble Fe(II) accumulations in Catalina Island sediments. Fe(II) concentration measured (by Ferrozine assay) in 0.22 μm filtered supernatants from Catalina Island sediments incubated with oxidized PCA, reduced PCA, oxidized 1-OH-PHZ, reduced 1-OH-PHZ, or no addition. Data correspond to experiments conducted using sediments from Site 1 collected in August or from Site 2 collected in August and October. Box and whisker plots reflect data from 4 or 5 replicates, data points >1.5x the interquartile range are shown as single black dots. Fe(II) measurements are notably noisy and may reflect both dynamic re-adsorption at mineral surfaces as well as experimental artifacts due to interference from high concentrations Fe(III), a known problem with the Ferrozine assay (*54*).

Phyla	Species	Alt. Species Name Used in Tree	Metabolite	Type	Note	Citation
Actinobacteriota	*Corynebacterium hydrocarboclastus*	*Corynebacterium sp.*	corynecin	chloramphenicol		(*55*)
Actinobacteriota	*Nocardia lactamdurans*	*Amycolatopsis lactamdurans*	cephamycin	ß-lactam		(*56*)
Actinobacteriota	*Proactynomces fructiferi*		ristomycin	aminoglycoside		(*5*)
Actinobacteriota	*Proactynomces fructiferi var ristomycin*		ristomycin	aminoglycoside		(*5*)
Actinobacteriota	*Streptomyces acrimycini* JI2236		candicidin	polyene macrolide		(*57*)
Actinobacteriota	*Streptomyces antibioticus*		antimycin	antimycin		(*58*)
Actinobacteriota	*Streptomyces antibioticus*		oleandomycin	macrolide		(*5*)
Actinobacteriota	*Streptomyces aureofaciens*	*Kitasatospora aureofaciens*	ayfactin (AYE)	polyene macrolide		(*59*)
Actinobacteriota	*Streptomyces aureofaciens*	*Kitasatospora aureofaciens*	chlortetracycline	tetracycline		(*60*)
Actinobacteriota	*Streptomyces avermitilis*		avermectin	macrolide	PHO	(*61*)
Actinobacteriota	*Streptomyces cattleya*		thienamycin	ß -lactam		(*62*)
Actinobacteriota	*Streptomyces clavuligerus*		cephamycin	ß -lactam		(*63*)
Actinobacteriota	*Streptomyces clavuligerus*		clavulanic acid	ß -lactamase inhibitor		(*63*)
Actinobacteriota	*Streptomyces coelicolor* A3(2)		actinorhodin	benzoisochromanequinone		(*64*, *65*)
Actinobacteriota	*Streptomyces coelicolor* A3(2)		undecylprodigiosin	prodiginines (tripyrrole)		(*64*)
Actinobacteriota	*Streptomyces coelicolor* M145		actinorhodin	benzoisochromanequinone	PHO	(*66*, *67*)
Actinobacteriota	*Streptomyces coelicolor* M145		prodigiosin	prodiginines (tripyrrole)	PHO	(*66*, *67*)
Actinobacteriota	*Streptomyces fradiae*		neomycin	aminoglycoside		(*5*)
Actinobacteriota	*Streptomyces fradiae*		tylosin	macrolide		(*68*)
Actinobacteriota	*Streptomyces griseolus*		A9145 (sinefungin)	nucleoside		(*69*)
Actinobacteriota	*Streptomyces griseus*		candicidin	polyene macrolide	PHO likely	(*70*) PHO: (*71*, *72*)
Actinobacteriota	*Streptomyces griseus*		cyclohexamide	glutarimide		(*73*)
Actinobacteriota	*Streptomyces griseus*		grixazone	phenoxazine		(*74*)
Actinobacteriota	*Streptomyces griseus*		streptomycin	aminoglycoside		(*75*)
Actinobacteriota	*Streptomyces hygroscopicus*		geldanamycin	benzoquinone	PHO	(*76*)
Actinobacteriota	*Streptomyces jamaicensis*		monamycin	cyclic depsipeptide		(*77*)
Actinobacteriota	*Streptomyces kanamyceticus*		kanamycin	aminoglycoside		(*78*)
Actinobacteriota	*Streptomyces levoris*		levorin	polyene macrolide		(*79*)
Actinobacteriota	*Streptomyces lividans*		actinorhodin	benzoisochromanequinone	PHO	(*24*)
Actinobacteriota	*Streptomyces lividans*		undecylprodigiosin	prodiginines (tripyrrole)	PHO	(*24*)
Actinobacteriota	*Streptomyces natalensis*		pimaricin (natamycin)	polyene macrolide	PHO	(*80*)
Actinobacteriota	*Streptomyces niveus*		novobiocin (albamycin, cathomycin)	aminocoumarin		(*81*)
Actinobacteriota	*Streptomyces nodusus*	*Streptomyces nodosus*	amphotericin	polyene macrolide		(*5*)
Actinobacteriota	*Streptomyces noursei*		nourseothricin	aminoglycoside		(*82*)

Actinobacteriota	*Streptomyces noursei*		nystatin	polyene macrolide		(*5*)
Actinobacteriota	*Streptomyces orientalis*	*Amycolatopsis orientalis*	vancomycin	glycopeptide		(*83*)
Actinobacteriota	*Streptomyces rimosus*		oxytetracycline	tetracycline	PHO likely	(*84*) PHO: (*85*)
Actinobacteriota	*Streptomyces rosa*		nanomycin	benzoisochromanequinone		(*86*)
Actinobacteriota	*Streptomyces tendae*		nikkomycin	petidyl nucleoside		(*87*)
Actinobacteriota	*Streptomyces tsukubaensis*	*Streptomyces tsukubensis*	tacrolimus	macrolide		(*88*)
Actinobacteriota	*Streptomyces venezuelae*		jadomycin	benzoxazolophenanthridine		(*89*)
Actinobacteriota	*Streptomyces viridoflavus*		candidin	polyene macrolide		(*5*)
Actinobacteriota	*Streptoverticillium mycoheptinicum*		mycoheptin	polyene macrolide		(*5*)
Actinobacteriota	*Streptoverticillium rimofaciens*		mildiomycin	nucleoside		(*90*)
Firmicutes	*Bacillus brevis*	*Aneurinibacillus migulanus*	gramicidin S	polypeptide		(*91*)
Firmicutes	*Bacillus circulans*		butirosin	aminoglycoside		(*5*)
Firmicutes	*Bacillus licheniformis*		bacitracin	polypeptide		(*92*)
Firmicutes	*Bacillus polymyxa*	*Paenibacillus polymyxa*	polymyxin (colistin)	polypeptide		(*93*)
Proteobacteria	*Burkholderia thailandensis* E-264		bactobolin	actinobolin/bactobolin		This study: Fig. S1
Proteobacteria	*Dyella japonica*		myxin	phenazine		(*27*)
Proteobacteria	*Pseudomonas aeruginosa*		pyocyanin	phenazine		(*19*)
Proteobacteria	*Pseudomonas aeruginosa* ATCC10145		pyocyanin	phenazine		(*4*)
Proteobacteria	*Pseudomonas aeruginosa* PAO1		pyocyanin	phenazine		(*21*)
Proteobacteria	*Pseudomonas aeruginosa* SCV 20265		pyocyanin	phenazine	PHO	(*23*)
Proteobacteria	*Pseudomonas chlororaphis* P3		phenazine-1-carboxamide	phenazine		(*22*)
Proteobacteria	*Pseudomonas chlororaphis* PCL1391		phenazine-1-carboxamide	phenazine		(*94*)
Proteobacteria	*Pseudovibrio* sp. FO-BEG1		tropodithietic acid	tropolone		(*95*)
Proteobacteria	*Serratia* ATCC39006		carbapenem	ß -lactam	PHO	(*53, 96*)
Proteobacteria	*Serratia* ATCC39006		prodigiosin	prodiginines (tripyrrole)	PHO	This study: Fig. S1, PHO:(*53, 96*)
Proteobacteria	*Serratia marcescens*		prodigiosin	prodiginines (tripyrrole)		(*52*)

Table S1. Species with documented P regulation of secondary metabolite production. In some cases, a reference to a compilation (*5*) is given when original papers could not be independently verified. Some species did not have representative sequences in the SILVA database and are absent from Fig. 1A. "PHO" indicates experimental evidence for involvement of *phoB*/*P* or *phoR* in metabolite production. "PHO likely" indicates experimental verification of PHO box transcription without direct verification of *phoB/P* or *phoR* involvement.

Name	Description	Source
Wild type strains		
Burkholderia thailandensis E264	Wild type	DSM 13276
Dyella japonica UNC79MFTsu3.2	Wild type	(*97*)
P. aeruginosa UCBPP-PA14	Wild type	DKN263
P. aureofaciens 30-84	Wild type	DKN183
P. chlororaphis PCL1391	Wild type	DKN100
P. fluorescens 2-79	Wild type	DKN240
Serratia ATCC39006	Wild type	ATCC39006
Deletion strains		
Dyella japonica UNC79MFTsu3.2	Δ*phzT*	(*27*)
P. aeruginosa UCBPP-PA14	Δ*phzA-G1*, Δ*phzA-G2*	(*47*)
P. chlororaphis PCL1391	Δ*phoB*	This study
P. chlororaphis PCL1391	Δ*phoB* complemented at the *att*Tn7 site	This study
P. fluorescens 2-79	Δ*phoB*	This study
P. fluorescens 2-79	Δ*phoB* complemented at the *att*Tn7 site	This study
***E. coli* strains**		
DH10B	Used for routine cloning	
SM10 λpir	Helper strain (carries pTNS1)	(*42*)
HB101	Helper strain (carries pRK2013)	(*42*)
Plasmids		
pMQ30	Conjugal vector for making unmarked deletions	(*40*)
pRK2013	Helper plasmid for integration at *att*Tn7 site and for unmarked deletions (carried by HB101)	(*42*)
pTNS1	Helper plasmid for integration at *att*Tn7 site (carried by SM10 λpir)	(*42*)
pUC18T-mini-Tn7T-Gm^R	Conjugal vector for integration at *att*Tn7 site	(*42*)

Table S2. Strains and plasmids used in this study.

Name	Sequence 5´-3´	Description	Purpose
PC *phoB* Upstream Fwd	ttttcccagtcacgacgttgtaaaacgacggccagtgccaTGGTGCTGGGCGCAGCGT	LC: overlap with PMQ30, UC: complementary to 5´ of *P. chlororaphis phoB* upstream region	Generating *P. chlororaphis* Δ*phoB*
PC *phoB* Upstream Rev	tggcgaataaggggccggctGCTTAATCCTCTTGTCATTTAACTGTCTTGCGCCG	LC: overlap with downstream region, UC: complementary to 3´ of *P. chlororaphis phoB* upstream region	Generating *P. chlororaphis* Δ*phoB*
PC *phoB* Downstream Fwd	aaatgacaagaggattaagcAGCCGGCCCCTTATTCGC	LC: overlap with upstream region, UC: complementary to 5´ of *P. chlororaphis phoB* downstream region	Generating *P. chlororaphis* Δ*phoB*
PC *phoB* Downstream Rev	acacaggaaacagctatgaccatgattacgaattcgagctCTCGGCGGGGGTGTATTTC	LC: overlap with PMQ30, UC: complementary to 3´ of *P. chlororaphis phoB* downstream region	Generating *P. chlororaphis* Δ*phoB*
PC *phoB* F	aattcgatcatgcatgagctGCGCAGCGCTCAGCAACA	LC: overlap with pUC18T-mini-Tn7T, UC: complementary to *P. chlororaphis phoB* promoter region	Complementing *P. chlororaphis* Δ*phoB*
PC *phoB* R	ttcgcgaggtaccgggcccaTTAACACGCGTCCTTGTAAGCGTC	LC: overlap with pUC18T-mini-Tn7T, UC: complementary to *P. chlororaphis phoB* downstream region	Complementing *P. chlororaphis* Δ*phoB*
PF *phoB* Upstream Fwd	ttttcccagtcacgacgttgtaaaacgacggccagtgccaGGGCATGCCGATGGCATTTAC	LC: overlap with PMQ30, UC: complementary to 5´ of *P. fluorescens phoB* upstream region	Generating *P. fluorescens* Δ*phoB*
PF *phoB* Upstream Rev	taagggaggggagggctggcGCCTAAAATCCTCTTGTCATTTAACTGTC	LC: overlap with downstream region, UC: complementary to 3´ of *P. fluorescens phoB* upstream region	Generating *P. fluorescens* Δ*phoB*
PF *phoB* Downstream Fwd	atgacaagaggattttaggcGCCAGCCCTCCCCTCCCT	LC: overlap with upstream region, UC: complementary to 5´ of *P. fluorescens phoB* downstream region	Generating *P. fluorescens* Δ*phoB*
PF *phoB* Downstream Rev	acacaggaaacagctatgaccatgattacgaattcgagctGTACTTCACCGCGTTGAACACCAGG	LC: overlap with PMQ30, UC: complementary to 3´ of *P. fluorescens phoB* downstream region	Generating *P. fluorescens* Δ*phoB*
PF *phoB* F	aattcgatcatgcatgagctCCGCCGTAACCAGCAGGG	LC: overlap with pUC18T-mini-Tn7T, UC: complementary to *P. fluorescens phoB* promoter region	Complementing *P. fluorescens* Δ*phoB*
PF *phoB* R	ttcgcgaggtaccgggcccaTTAAACATGCGTCCTTGTCAGCTG	LC: overlap with pUC18T-mini-Tn7T, UC: complementary to *P. fluorescens phoB* downstream region	Complementing *P. fluorescens* Δ*phoB*

Table S3. Primers used in strain construction.

References and Notes

1. J. Davies, K. S. Ryan, Introducing the parvome: Bioactive compounds in the microbial world. *ACS Chem. Biol.* **7**, 252–259 (2012). doi:10.1021/cb200337h Medline

2. A. L. Demain, A. Fang, in *History of Modern Biotechnolog*, A. Fietcher, Ed. (Springer, 2000), pp. 1–39.

3. A. Price-Whelan, L. E. P. Dietrich, D. K. Newman, Rethinking 'secondary' metabolism: Physiological roles for phenazine antibiotics. *Nat. Chem. Biol.* **2**, 71–78 (2006). doi:10.1038/nchembio764 Medline

4. M. A. Whooley, A. J. McLoughlin, The regulation of pyocyanin production in *Pseudomonas aeruginosa*. *Eur. J. Appl. Microbiol. Biotechnol.* **15**, 161–166 (1982). doi:10.1007/BF00511241

5. J. F. Martín, in *Advances in Biochemical Engineering* (Springer, 1977), vol. 6, pp. 105–127.

6. F. Santos-Beneit, The Pho regulon: A huge regulatory network in bacteria. *Front. Microbiol.* **6**, 402 (2015). doi:10.3389/fmicb.2015.00402 Medline

7. P. N. Froelich, M. L. Bender, N. A. Luedtke, G. R. Heath, T. DeVries, The marine phosphorus cycle. *Am. J. Sci.* **282**, 474–511 (1982). doi:10.2475/ajs.282.4.474

8. P. Van Cappellen, E. D. Ingall, Redox stabilization of the atmosphere and oceans by phosphorus-limited marine productivity. *Science* **271**, 493–496 (1996). doi:10.1126/science.271.5248.493 Medline

9. M. Obersteiner, J. Peñuelas, P. Ciais, M. van der Velde, I. A. Janssens, The phosphorus trilemma. *Nat. Geosci.* **6**, 897–898 (2013). doi:10.1038/ngeo1990

10. E. Du, C. Terrer, A. F. A. Pellegrini, A. Ahlström, C. J. van Lissa, X. Zhao, N. Xia, X. Wu, R. B. Jackson, Global patterns of terrestrial nitrogen and phosphorus limitation. *Nat. Geosci.* **13**, 221–226 (2020). doi:10.1038/s41561-019-0530-4

11. H. Rodríguez, R. Fraga, Phosphate solubilizing bacteria and their role in plant growth promotion. *Biotechnol. Adv.* **17**, 319–339 (1999). doi:10.1016/S0734-9750(99)00014-2 Medline

12. A. Canarini, C. Kaiser, A. Merchant, A. Richter, W. Wanek, Root exudation of primary metabolites: Mechanisms and their roles in plant responses to environmental stimuli. *Front. Plant Sci.* **10**, 157 (2019). doi:10.3389/fpls.2019.00157 Medline

13. S. A. Crosby, G. E. Millward, E. I. Butler, D. R. Turner, M. Whitfield, Kinetics of phosphate adsorption by iron oxyhydroxides in aqueous systems. *Estuar. Coast. Shelf Sci.* **19**, 257–270 (1984). doi:10.1016/0272-7714(84)90069-6

14. T. Borch, S. Fendorf, in *Adsorption of Metals by Geomedia II*, vol. 7 of *Developments in Earth and Environmental Science*, M. O. Barnett, D. B. Kent, Eds. (Elsevier, 2008), chap. 12, pp. 321–348.

15. T. Peretyazhko, G. Sposito, Iron(III) reduction and phosphorous solubilization in humid tropical forest soils. *Geochim. Cosmochim. Acta* **69**, 3643–3652 (2005). doi:10.1016/j.gca.2005.03.045

16. E. D. Brutinel, J. A. Gralnick, Shuttling happens: Soluble flavin mediators of extracellular electron transfer in *Shewanella*. *Appl. Microbiol. Biotechnol.* **93**, 41–48 (2012). doi:10.1007/s00253-011-3653-0 Medline

17. Y. Wang, D. K. Newman, Redox reactions of phenazine antibiotics with ferric (hydr)oxides and molecular oxygen. *Environ. Sci. Technol.* **42**, 2380–2386 (2008). doi:10.1021/es702290a Medline

18. N. R. Glasser, S. H. Saunders, D. K. Newman, The colorful world of extracellular electron shuttles. *Annu. Rev. Microbiol.* **71**, 731–751 (2017). doi:10.1146/annurev-micro-090816-093913 Medline

19. M. O. Burton, J. J. Campbell, B. A. Eagles, The mineral requirements for pyocyanin production. *Can. J. Res.* **26**, 15–22 (1948). Medline

20. H. Sakhtah, A. Price-Whelan, L. E. P. Dietrich, in *Microbial Phenazines: Biosynthesis, Agriculture and Health*, S. Chincholkar, L. S. Thomashow, Eds. (Springer, 2013), pp. 19–42.

21. B. Mellbye, M. Schuster, Physiological framework for the regulation of quorum sensing-dependent public goods in *Pseudomonas aeruginosa*. *J. Bacteriol.* **196**, 1155–1164 (2014). doi:10.1128/JB.01223-13 Medline

22. X.-J. Jin, H.-S. Peng, H.-B. Hu, X.-Q. Huang, W. Wang, X.-H. Zhang, iTRAQ-based quantitative proteomic analysis reveals potential factors associated with the enhancement of phenazine-1-carboxamide production in *Pseudomonas chlororaphis* P3. *Sci. Rep.* **6**, 27393 (2016). doi:10.1038/srep27393 Medline

23. V. Jensen, D. Löns, C. Zaoui, F. Bredenbruch, A. Meissner, G. Dieterich, R. Münch, S. Häussler, RhlR expression in *Pseudomonas aeruginosa* is modulated by the *Pseudomonas* quinolone signal via PhoB-dependent and -independent pathways. *J. Bacteriol.* **188**, 8601–8606 (2006). doi:10.1128/JB.01378-06 Medline

24. A. Sola-Landa, R. S. Moura, J. F. Martín, The two-component PhoR-PhoP system controls both primary metabolism and secondary metabolite biosynthesis in *Streptomyces lividans*. *Proc. Natl. Acad. Sci. U.S.A.* **100**, 6133–6138 (2003). doi:10.1073/pnas.0931429100 Medline

25. D. V. Mavrodi, O. V. Mavrodi, J. A. Parejko, R. F. Bonsall, Y.-S. Kwak, T. C. Paulitz, L. S. Thomashow, D. M. Weller, Accumulation of the antibiotic phenazine-1-carboxylic acid in the rhizosphere of dryland cereals. *Appl. Environ. Microbiol.* **78**, 804–812 (2012). doi:10.1128/AEM.06784-11 Medline

26. L. Zhang, X. Tian, S. Kuang, G. Liu, C. Zhang, C. Sun, Antagonistic activity and mode of action of phenazine-1-carboxylic acid, produced by marine bacterium *Pseudomonas aeruginosa* PA31x, against *Vibrio anguillarum in vitro* and in a zebrafish *in vivo* model. *Front. Microbiol.* **8**, 289 (2017). doi:10.3389/fmicb.2017.00289 Medline

27. D. Dar, L. S. Thomashow, D. M. Weller, D. K. Newman, Global landscape of phenazine biosynthesis and biodegradation reveals species-specific colonization patterns in agricultural soils and crop microbiomes. *eLife* **9**, e59726 (2020). doi:10.7554/eLife.59726 Medline

28. A. R. Rowe, P. Chellamuthu, B. Lam, A. Okamoto, K. H. Nealson, Marine sediments microbes capable of electrode oxidation as a surrogate for lithotrophic insoluble substrate metabolism. *Front. Microbiol.* **5**, 784 (2015). doi:10.3389/fmicb.2014.00784 Medline

29. W. Stumm, B. Sulzberger, The cycling of iron in natural environments: Considerations based on laboratory studies of heterogenous redox processes. *Geochim. Cosmochim. Acta* **56**, 3233–3257 (1992). doi:10.1016/0016-7037(92)90301-X

30. P. V. Sundareshwar, J. T. Morris, E. K. Koepfler, B. Fornwalt, Phosphorus limitation of coastal ecosystem processes. *Science* **299**, 563–565 (2003). doi:10.1126/science.1079100 Medline

31. T. Wu, Q. Xue, F. Liu, J. Zhang, C. Zhou, J. Cao, H. Chen, Mechanistic insight into interactions between tetracycline and two iron oxide minerals with different crystal structures. *Chem. Eng. J.* **366**, 577–586 (2019). doi:10.1016/j.cej.2019.02.128

32. K. M. Dahlstrom, D. L. McRose, D. K. Newman, Keystone metabolites of crop rhizosphere microbiomes. *Curr. Biol.* **30**, R1131–R1137 (2020). doi:10.1016/j.cub.2020.08.005 Medline

33. A. Stamatakis, RAxML-VI-HPC: Maximum likelihood-based phylogenetic analyses with thousands of taxa and mixed models. *Bioinformatics* **22**, 2688–2690 (2006). doi:10.1093/bioinformatics/btl446 Medline

34. F. O. Glöckner, P. Yilmaz, C. Quast, J. Gerken, A. Beccati, A. Ciuprina, G. Bruns, P. Yarza, J. Peplies, R. Westram, W. Ludwig, 25 years of serving the community with ribosomal RNA gene reference databases and tools. *J. Biotechnol.* **261**, 169–176 (2017). doi:10.1016/j.jbiotec.2017.06.1198 Medline

35. E. Pruesse, J. Peplies, F. O. Glöckner, SINA: Accurate high-throughput multiple sequence alignment of ribosomal RNA genes. *Bioinformatics* **28**, 1823–1829 (2012). doi:10.1093/bioinformatics/bts252 Medline

36. I. Letunic, P. Bork, Interactive Tree Of Life (iTOL) v4: Recent updates and new developments. *Nucleic Acids Res.* **47**, W256–W259 (2019). doi:10.1093/nar/gkz239 Medline

37. W. G. Sunda, N. M. Price, F. M. M. Morel, in *Algal Culturing Techniques*, R. A. Andersen, Ed. (Elsevier Academic Press, 2005), pp. 35–63.

38. A. C. Redfield, in *James Johnstone Memorial Volume*, R. J. Daniel, Ed. (University Press of Liverpool, 1934), pp. 176–192.

39. M. R. Seyedsayamdost, J. R. Chandler, J. A. V. Blodgett, P. S. Lima, B. A. Duerkop, K. Oinuma, E. P. Greenberg, J. Clardy, Quorum-sensing-regulated bactobolin production by *Burkholderia thailandensis* E264. *Org. Lett.* **12**, 716–719 (2010). doi:10.1021/ol902751x Medline

40. R. M. Q. Shanks, N. C. Caiazza, S. M. Hinsa, C. M. Toutain, G. A. O'Toole, *Saccharomyces cerevisiae*-based molecular tool kit for manipulation of genes from gram-negative bacteria. *Appl. Environ. Microbiol.* **72**, 5027–5036 (2006). doi:10.1128/AEM.00682-06 Medline

41. D. G. Gibson, L. Young, R.-Y. Chuang, J. C. Venter, C. A. Hutchison 3rd, H. O. Smith, Enzymatic assembly of DNA molecules up to several hundred kilobases. *Nat. Methods* **6**, 343–345 (2009). doi:10.1038/nmeth.1318 Medline

42. K.-H. Choi, H. P. Schweizer, mini-Tn7 insertion in bacteria with single attTn7 sites: Example *Pseudomonas aeruginosa*. *Nat. Protoc.* **1**, 153–161 (2006). doi:10.1038/nprot.2006.24 Medline

43. U. Schwertmann, R. M. Cornell, *Iron Oxides in the Laboratory: Preparation and Characterization*. (Wiley-VCH, 2000).

44. X. Wang, W. Li, R. Harrington, F. Liu, J. B. Parise, X. Feng, D. L. Sparks, Effect of ferrihydrite crystallite size on phosphate adsorption reactivity. *Environ. Sci. Technol.* **47**, 10322–10331 (2013). doi:10.1021/es401301z Medline

45. M. Mallet, K. Barthélémy, C. Ruby, A. Renard, S. Naille, Investigation of phosphate adsorption onto ferrihydrite by X-ray photoelectron spectroscopy. *J. Colloid Interface Sci.* **407**, 95–101 (2013). doi:10.1016/j.jcis.2013.06.049 Medline

46. L. L. Stookey, Ferrozine–a new spectrophotometric reagent for iron. *Anal. Chem.* **42**, 779–781 (1970). doi:10.1021/ac60289a016

47. L. E. P. Dietrich, A. Price-Whelan, A. Petersen, M. Whiteley, D. K. Newman, The phenazine pyocyanin is a terminal signalling factor in the quorum sensing network of *Pseudomonas aeruginosa*. *Mol. Microbiol.* **61**, 1308–1321 (2006). doi:10.1111/j.1365-2958.2006.05306.x Medline

48. G. Chowdhury, U. Sarkar, S. Pullen, W. R. Wilson, A. Rajapakse, T. Fuchs-Knotts, K. S. Gates, DNA strand cleavage by the phenazine di-N-oxide natural product myxin under both aerobic and anaerobic conditions. *Chem. Res. Toxicol.* **25**, 197–206 (2012). doi:10.1021/tx2004213 Medline

49. N. L. Sullivan, D. S. Tzeranis, Y. Wang, P. T. C. So, D. Newman, Quantifying the dynamics of bacterial secondary metabolites by spectral multiphoton microscopy. *ACS Chem. Biol.* **6**, 893–899 (2011). doi:10.1021/cb200094w Medline

50. J. D. Cline, Spectrophotometric determination of hydrogen sulfide in natural waters. *Limnol. Oceanogr.* **14**, 454–458 (1969). doi:10.4319/lo.1969.14.3.0454

51. RCoreTeam, The R Project for Statistical Computing (R Foundation for Statistical Computing, Vienna, Austria, 2020); www.r-project.org/.

52. F. R. Witney, M. L. Failla, E. D. Weinberg, Phosphate inhibition of secondary metabolism in *Serratia marcescens*. *Appl. Environ. Microbiol.* **33**, 1042–1046 (1977). doi:10.1128/AEM.33.5.1042-1046.1977 Medline

53. H. Slater, M. Crow, L. Everson, G. P. C. Salmond, Phosphate availability regulates biosynthesis of two antibiotics, prodigiosin and carbapenem, in *Serratia* via both quorum-sensing-dependent and -independent pathways. *Mol. Microbiol.* **47**, 303–320 (2003). doi:10.1046/j.1365-2958.2003.03295.x Medline

54. J. Im, J. Lee, F. E. Löffler, Interference of ferric ions with ferrous iron quantification using the ferrozine assay. *J. Microbiol. Methods* **95**, 366–367 (2013). doi:10.1016/j.mimet.2013.10.005 Medline

55. H. Nakano, F. Tomita, K. Yamaguchi, M. Nagashima, T. Suzuki, Corynecin (chloramphenicol analogs) fermentation studies: Selective production of Corynecin I by *Corynebacterium hydrocarboclastus* grown on acetate. *Biotechnol. Bioeng.* **19**, 1009–1018 (1977). doi:10.1002/bit.260190705 Medline

56. A. C. Kirpekar, D. J. Kirwan, R. W. Stieber, Effects of glutamate, glucose, phosphate, and alkali metal ions on cephamycin C production by *Nocardia lactamdurans* in defined media. *Biotechnol. Bioeng.* **38**, 1100–1109 (1991). doi:10.1002/bit.260380919 Medline

57. J. A. Asturias, J. F. Martín, P. Liras, Biosynthesis and phosphate control of candicidin by *Streptomyces acrimycini* JI2236: Effect of amplification of the pabAB gene. *J. Ind. Microbiol.* **13**, 183–189 (1994). doi:10.1007/BF01584005 Medline

58. M. Raman Kutty, L. V. Kannan, Z. Rehacek, Effect of phosphate on biosynthesis of antimycin A and production and utilization of poly-beta-hydroxybutyrate by *Streptomyces antibioticus*. *Indian J. Biochem.* **6**, 230–231 (1969). Medline

59. A.-Z. A. Abou-Zeid, A.-S. Y. Abou-el-Atta, The antifungal antibiotic (AYE) produced by *Streptomyces aureofaciens. Zentral. Bakteriol. Naturwiss.* **126**, 371–375 (1970).

60. A. Prokofieva-Belgovskaya, L. Popova, The influence of phosphorus on the development of *Streptomyces aureofaciens* and on its ability to produce chlortetracycline. *J. Gen. Microbiol.* **20**, 462–472 (1959). doi:10.1099/00221287-20-3-462 Medline

61. R. Yang, X. Liu, Y. Wen, Y. Song, Z. Chen, J. Li, The PhoP transcription factor negatively regulates avermectin biosynthesis in *Streptomyces avermitilis*. *Appl. Microbiol. Biotechnol.* **99**, 10547–10557 (2015). doi:10.1007/s00253-015-6921-6 Medline

62. G. Lilley, A. E. Clark, G. C. Lawrence, Control of the production of cephamycin C and thienamycin by *Streptomyces cattleya* NRRL 8057. *J. Chem. Technol. Biotechnol.* **31**, 127–134 (1981). doi:10.1002/jctb.280310118

63. A. Lebrihi, P. Germain, G. Lefebvre, Phosphate repression of cephamycin and clavulanic acid production by *Streptomyces clavuligerus*. *Appl. Microbiol. Biotechnol.* **26**, 130–135 (1987). doi:10.1007/BF00253896

64. G. Hobbs, C. M. Frazer, D. C. J. Gardner, F. Flett, S. G. Oliver, Pigmented antibiotic production by *Streptomyces coelicolor* A3(2): Kinetics and the influence of nutrients. *Microbiology* **136**, 2291–2296 (1990).

65. J. L. Doull, L. C. Vining, Nutritional control of actinorhodin production by *Streptomyces coelicolor* A3(2): Suppressive effects of nitrogen and phosphate. *Appl. Microbiol. Biotechnol.* **32**, 449–454 (1990). doi:10.1007/BF00903781 Medline

66. F. Santos-Beneit, A. Rodríguez-García, A. Sola-Landa, J. F. Martín, Cross-talk between two global regulators in *Streptomyces*: PhoP and AfsR interact in the control of afsS, pstS and phoRP transcription. *Mol. Microbiol.* **72**, 53–68 (2009). doi:10.1111/j.1365-2958.2009.06624.x Medline

67. L. Thomas, D. A. Hodgson, A. Wentzel, K. Nieselt, T. E. Ellingsen, J. Moore, E. R. Morrissey, R. Legaie, W. Wohlleben, A. Rodríguez-García, J. F. Martín, N. J. Burroughs, E. M. H. Wellington, M. C. M. Smith; STREAM Consortium, Metabolic switches and adaptations deduced from the proteomes of Streptomyces coelicolor wild type and phoP

mutant grown in batch culture. *Mol. Cell. Proteomics* **11**, 013797 (2012). doi:10.1074/mcp.M111.013797 Medline

68. K. Vu-Trong, S. Bhuwapathanapun, P. P. Gray, Metabolic regulation in tylosin-producing *Streptomyces fradiae*: Phosphate control of tylosin biosynthesis. *Antimicrob. Agents Chemother.* **19**, 209–212 (1981). doi:10.1128/AAC.19.2.209 Medline

69. L. D. Boeck, G. M. Clem, M. M. Wilson, J. E. Westhead, A9145, a new adenine-containing antifungal antibiotic: Fermentation. *Antimicrob. Agents Chemother.* **3**, 49–56 (1973). doi:10.1128/AAC.3.1.49 Medline

70. P. Liras, J. R. Villanueva, J. F. Martín, Sequential expression of macromolecule biosynthesis and candicidin formation in *Streptomyces griseus*. *J. Gen. Microbiol.* **102**, 269–277 (1977). Medline

71. P. Liras, J. A. Asturias, J. F. Martín, Phosphate control sequences involved in transcriptional regulation of antibiotic biosynthesis. *Trends Biotechnol.* **8**, 184–189 (1990). doi:10.1016/0167-7799(90)90170-3 Medline

72. A. Rebollo, J. A. Gil, P. Liras, J. A. Asturias, J. F. Martín, Cloning and characterization of a phosphate-regulated promoter involved in phosphate control of candicidin biosynthesis. *Gene* **79**, 47–58 (1989). doi:10.1016/0378-1119(89)90091-7 Medline

73. A.-Z. A. Abou Zeid, Production of cycloheximide by *Streptomyces* sp. *Acta Microbiol. Pol. B* **4**, 83–88 (1972). Medline

74. Y. Ohnishi, Y. Furusho, T. Higashi, H.-K. Chun, K. Furihata, S. Sakuda, S. Horinouchi, Structures of grixazone A and B, A-factor-dependent yellow pigments produced under phosphate depletion by *Streptomyces griseus*. *J. Antibiot. (Tokyo)* **57**, 218–223 (2004). doi:10.7164/antibiotics.57.218 Medline

75. D. Perlman, G. H. Wagman, Studies on the utilization of lipids by *Streptomyces griseus*. *J. Bacteriol.* **63**, 253–262 (1952). doi:10.1128/JB.63.2.253-262.1952 Medline

76. J. F. Martín, A. Ramos, P. Liras, Regulation of geldanamycin biosynthesis by cluster-situated transcription factors and the master regulator PhoP. *Antibiotics (Basel)* **8**, 87 (2019). doi:10.3390/antibiotics8030087 Medline

77. M. J. Hall, C. H. Hassall, Production of the monamycins, novel depsipeptide antibiotics. *Appl. Microbiol.* **19**, 109–112 (1970). doi:10.1128/AM.19.1.109-112.1970 Medline

78. K. Basak, S. K. Majumdar, Mineral nutrition of *Streptomyces kanamyceticus* for kanamycin formation. *Antimicrob. Agents Chemother.* **8**, 391–395 (1975). doi:10.1128/AAC.8.4.391 Medline

79. M. L. Zyuzina, T. P. Efimova, Effect of inorganic phosphate on levorin biosynthesis and composition of *Streptomyces levoris* mycelium. *Antibiotiki* **24**, 656–659 (1979). Medline

80. M. V. Mendes, S. Tunca, N. Antón, E. Recio, A. Sola-Landa, J. F. Aparicio, J. F. Martín, The two-component *phoR-phoP* system of *Streptomyces natalensis*: Inactivation or deletion of phoP reduces the negative phosphate regulation of pimaricin biosynthesis. *Metab. Eng.* **9**, 217–227 (2007). doi:10.1016/j.ymben.2006.10.003 Medline

81. H. Hoeksema, C. G. Smith, Novobiocin. *Prog. Ind. Microbiol.* **3**, 91–139 (1961). Medline

82. P. J. Müller, G. Haubold, M. Menner, H. H. Grosse, J. H. Ozegowski, H. Bocker, Effect of phosphate on the biosynthesis of nourseothricin by Streptomyces noursei JA 3890b. *Z. Allg. Mikrobiol.* **24**, 555–564 (1984). doi:10.1002/jobm.3630240812 Medline

83. F. P. Mertz, L. E. Doolin, The effect of inorganic phosphate on the biosynthesis of vancomycin. *Can. J. Microbiol.* **19**, 263–270 (1973). doi:10.1139/m73-040 Medline

84. W. A. Zygmunt, Influence of inorganic phosphorus on oxytetracycline formation by *Streptomyces rimosus*. *Appl. Microbiol.* **12**, 195–196 (1964). doi:10.1128/AM.12.3.195-196.1964 Medline

85. K. J. McDowall, A. Thamchaipenet, I. S. Hunter, Phosphate control of oxytetracycline production by *Streptomyces rimosus* is at the level of transcription from promoters overlapped by tandem repeats similar to those of the DNA-binding sites of the OmpR family. *J. Bacteriol.* **181**, 3025–3032 (1999). doi:10.1128/JB.181.10.3025-3032.1999 Medline

86. R. Masuma, Y. Tanaka, H. Tanaka, S. Omura, Production of nanaomycin and other antibiotics by phosphate-depressed fermentation using phosphate-trapping agents. *J. Antibiot. (Tokyo)* **39**, 1557–1564 (1986). doi:10.7164/antibiotics.39.1557 Medline

87. D. Hege-Treskatis, R. King, H. Wolf, E.-D. Gilles, Nutritional control of nikkomycin and juglomycin production by *Streptomyces tendae* in continuous culture. *Appl. Microbiol. Biotechnol.* **36**, 440–445 (1992). doi:10.1007/BF00170179 Medline

88. M. Martínez-Castro, Z. Salehi-Najafabadi, F. Romero, R. Pérez-Sanchiz, R. I. Fernández-Chimeno, J. F. Martín, C. Barreiro, Taxonomy and chemically semi-defined media for the analysis of the tacrolimus producer '*Streptomyces tsukubaensis*'. *Appl. Microbiol. Biotechnol.* **97**, 2139–2152 (2013). doi:10.1007/s00253-012-4364-x Medline

89. D. L. Jakeman, C. L. Graham, W. Young, L. C. Vining, Culture conditions improving the production of jadomycin B. *J. Ind. Microbiol. Biotechnol.* **33**, 767–772 (2006). doi:10.1007/s10295-006-0113-4 Medline

90. K. Kishimoto, Y. S. Park, M. Okabe, S. Akiyama, Effect of phosphate ion on mildiomycin production by *Streptoverticillium rimofaciens*. *J. Antibiot. (Tokyo)* **49**, 775–780 (1996). doi:10.7164/antibiotics.49.775 Medline

91. E. J. Vandamme, A. L. Demain, Nutrition of *Bacillus brevis* ATCC 9999, the producer of gramicidin S. *Antimicrob. Agents Chemother.* **10**, 265–273 (1976). doi:10.1128/AAC.10.2.265 Medline

92. H. I. Haavik, Studies on the formation of bacitracin by *Bacillus licheniformis*: Effect of inorganic phosphate. *J. Gen. Microbiol.* **84**, 226–230 (1974). doi:10.1099/00221287-84-1-226 Medline

93. Y. Kuratsu, M. Sakurai, K. Inuzuka, T. Suzuki, Effect of phosphate ion and ammonia-nitrogen on colistin production by *Bacillus polymyxa*. *J. Ferment. Technol.* **61**, 365–371 (1983).

94. E. T. van Rij, M. Wesselink, T. F. C. Chin-A-Woeng, G. V. Bloemberg, B. J. J. Lugtenberg, Influence of environmental conditions on the production of phenazine-1-carboxamide by

Pseudomonas chlororaphis PCL1391. *Mol. Plant Microbe Interact.* **17**, 557–566 (2004). doi:10.1094/MPMI.2004.17.5.557 Medline

95. S. Romano, H. N. Schulz-Vogt, J. M. González, V. Bondarev, Phosphate limitation induces drastic physiological changes, virulence-related gene expression, and secondary metabolite production in *Pseudovibrio* sp. strain FO-BEG1. *Appl. Environ. Microbiol.* **81**, 3518–3528 (2015). doi:10.1128/AEM.04167-14 Medline

96. T. Gristwood, P. C. Fineran, L. Everson, N. R. Williamson, G. P. Salmond, The PhoBR two-component system regulates antibiotic biosynthesis in *Serratia* in response to phosphate. *BMC Microbiol.* **9**, 112 (2009). doi:10.1186/1471-2180-9-112 Medline

97. A. Levy, I. Salas Gonzalez, M. Mittelviefhaus, S. Clingenpeel, S. Herrera Paredes, J. Miao, K. Wang, G. Devescovi, K. Stillman, F. Monteiro, B. Rangel Alvarez, D. S. Lundberg, T.-Y. Lu, S. Lebeis, Z. Jin, M. McDonald, A. P. Klein, M. E. Feltcher, T. G. Rio, S. R. Grant, S. L. Doty, R. E. Ley, B. Zhao, V. Venturi, D. A. Pelletier, J. A. Vorholt, S. G. Tringe, T. Woyke, J. L. Dangl, Genomic features of bacterial adaptation to plants. *Nat. Genet.* **50**, 138–150 (2017). doi:10.1038/s41588-017-0012-9 Medline